Phase fluctuations in anisotropic Bose-Einstein condensates: From cigars to rings

L. Mathey, A. Ramanathan, K. C. Wright, S. R. Muniz, W. D. Phillips, and Charles W. Clark
Joint Quantum Institute, National Institute of Standards and Technology and University of Maryland, Gaithersburg, Maryland 20899, USA
(Received 1 July 2010; published 14 September 2010)

We study the phase-fluctuating condensate regime of ultracold atoms trapped in a ring-shaped trap geometry, which has been realized in recent experiments. We first consider a simplified box geometry, in which we identify the conditions to create a state that is dominated by thermal phase fluctuations, and then explore the experimental ring geometry. In both cases we demonstrate that the requirement for strong phase fluctuations can be expressed in terms of the total number of atoms and the geometric length scales of the trap only. For the ring-shaped trap we discuss the zero temperature limit in which a condensate is realized where the phase is fluctuating due to interactions and quantum fluctuations. We also address possible ways of detecting the phase-fluctuating regime in ring condensates.

DOI: 10.1103/PhysRevA.82.033607 PACS number(s): 03.75.Hh, 03.75.−b, 05.30.−d

Since the laboratory realization of Bose-Einstein condensates in ultracold atomic systems, their properties in different dimensions and geometries and the effect of quantum and thermal fluctuations have been interesting questions. In Refs. [1,2], it was pointed out that for an elongated, "cigar"-shaped condensate, a regime of strong thermal fluctuations can exist. Such a system is three-dimensional (3D) in the sense that its transverse dimensions are significantly larger than the healing length and the thermal de Broglie wavelength. However, the long-range behavior of the single-particle (field-field) correlation function $g_1(\mathbf{r}) \equiv \langle \psi^\dagger(0)\psi(\mathbf{r})\rangle$, with $\psi(\mathbf{r})$ being the single-particle operator, can be dominated by phase fluctuations along the longitudinal direction. This leads to an exponential decay with some correlation length l_ϕ, which is typical for a one-dimensional system at finite (nonzero) temperature. Because the many-body state combines these properties that are characteristic for 3D and one-dimensional (1D) systems, such a system can be considered to be of mixed dimensionality. When the correlation length l_ϕ is of the order of the system size or shorter, the condensate is said to be in the phase-fluctuating regime. In Refs. [3] and [4] the 1D-3D crossover was studied. In Ref. [5], a two-step condensation mechanism for the noninteracting system was pointed out. The phase-fluctuating regime of elongated condensates was first experimentally realized in Ref. [6], and then studied in further detail in Refs. [7–10]. We note that quantum fluctuations can lead to a phase-fluctuating condensate even at zero temperature, as we discuss in Sec. II B. However, here the decay of the correlation function is algebraic, and we find that the exponent is very small for the parameter regime of interest. The main focus of this article are thermal phase fluctuations.

In this paper we study the properties of a ring-shaped phase-fluctuating condensate. One way to create such a system is by using both a quasi-2D optical dipole trap formed from a sheet of light (see Ref. [11]), and a Laguerre-Gauss (LG) beam perpendicular to the plane of the sheet [12]. In such a setup, the atoms can form a condensate along the ring-shaped maximum of the combined intensities of the sheet trap and the LG beam. (A different approach was demonstrated in Ref. [13].) Other realizations of toroidal traps were reported in Refs. [14–16]. Here, we study under what circumstances the regime of thermal phase fluctuations can be reached for a condensate with a ring geometry.

In Sec. I, we first take the simplified case of a box geometry with periodic boundary conditions, with different box sizes along different axes, with one of them much larger than the others. In Sec. II we study the case of a ring-shaped condensate. In Sec. III we consider ways in which this state can be seen experimentally, and in Sec. IV we conclude.

I. BOX GEOMETRY

In this section we consider a condensate in a three-dimensional box with periodic boundary conditions, and dimensions X, Y, and Z. Our goal is to study the behavior of the single-particle correlation function for the dimensional crossover from three dimensions to one dimension. This correlation function can be used to identify the phase-fluctuating regime of the condensate.

We consider the regimes $Z \approx X,Y$ and $Z \gg X,Y$, using the calculational approach that is used in Refs. [1,2]. This Bogoliubov-de Gennes (BdG) approach is particularly useful for spatially inhomogeneous systems. However, we apply it to the box geometry as well, to allow for a clearer comparison between this case and the results for a ring geometry in Sec. II. We first calculate the BdG modes, and then consider the thermal occupation of these modes.

In a qualitative sense, the box geometry with periodic boundary conditions displays the main features of a Bose-Einstein condensate in elongated geometries. Because it is calculationally simpler, it will serve as the main system to understand the properties of fluctuating condensates. In Sec. II we derive the analogous properties for the spatially inhomogeneous case, and compare them to results of this section.

We consider an atomic ensemble of bosons of density $n = N/V$, where N is the total particle number, and the volume V is XYZ. These atoms are assumed to be weakly interacting via a contact interaction with strength $g = 4\pi\hbar^2 a/M$, where a is the scattering length, and M is the atomic mass. We then apply a BdG approach to describe the condensate and the excitations. The condensate is described by the well-known Gross-Pitaevskii (GP) equation, Ref. [17]:

$$\left(-\frac{\hbar^2\nabla^2}{2M} + g|\Psi_0|^2\right)\Psi_0 = \mu\Psi_0, \tag{1}$$

where Ψ_0 is the condensate wave function, and μ is the chemical potential. Within the Thomas-Fermi (TF) approximation (see Ref. [18]), Ψ_0 is given by

$$\Psi_0 = \sqrt{n_0}, \tag{2}$$

where $n_0 = N_0/V$ is the condensate density, and N_0 is the total number of atoms in the condensate. For the weak interactions considered here, the quantum depletion is small and $N_0 \approx N$. The Bogoliubov-de Gennes (BdG) equations [19] are given by

$$\left(-\frac{\hbar^2\nabla^2}{2M}\right)u_\nu + g|\Psi_0|^2(2u_\nu - v_\nu) = (\mu + E_\nu)u_\nu, \tag{3}$$

$$\left(-\frac{\hbar^2\nabla^2}{2M}\right)v_\nu + g|\Psi_0|^2(2v_\nu - u_\nu) = (\mu - E_\nu)v_\nu. \tag{4}$$

The fields u_ν and v_ν describe an excitation of energy E_ν. We note that for a phase-fluctuating condensate, this formalism should be interpreted as an expansion in the density around a finite value, and in the phase to quadratic order (see Ref. [20]). We introduce the rescaled quantities: $\bar{x} = x/X$, $\bar{y} = y/Y, \bar{z} = z/Z$, and $\zeta^2 = \hbar^2/(2M\mu L^2)$ where L is defined as $L = (XYZ)^{1/3}$. Our objective is to generate a consistent expansion in ζ. Written in these rescaled quantities, the GP equation (1) is given by

$$-\zeta^2\tilde{\nabla}^2\Psi_0 + \bar{n}_0\Psi_0 = \Psi_0, \tag{5}$$

where $\tilde{\nabla}^2$ is defined as

$$\tilde{\nabla}^2 = \frac{L^2}{X^2}\frac{\partial^2}{\partial\bar{x}^2} + \frac{L^2}{Y^2}\frac{\partial^2}{\partial\bar{y}^2} + \frac{L^2}{Z^2}\frac{\partial^2}{\partial\bar{z}^2}. \tag{6}$$

The reduced density $\bar{n}_0$ is given by $\bar{n}_0 = g|\Psi_0|^2/\mu$. We note that the TF solution is simply the zeroth order solution in ζ (i.e., $\bar{n}_0 = 1$). The rescaled BdG equations are

$$-\zeta^2\tilde{\nabla}^2u_\nu + \bar{n}_0(2u_\nu - v_\nu) = (1 + 2\zeta\epsilon_\nu)u_\nu \tag{7}$$

$$-\zeta^2\tilde{\nabla}^2v_\nu + \bar{n}_0(2v_\nu - u_\nu) = (1 - 2\zeta\epsilon_\nu)v_\nu, \tag{8}$$

where $2\zeta\epsilon_\nu = E_\nu/\mu$. We now define the fields $f_{\pm,\nu} \equiv u_\nu \pm v_\nu$. These fields are related to the phase and density fluctuations of excitation ν. In terms of these fields, the BdG equations [Eqs. (7) and (8)] are

$$-\zeta^2\tilde{\nabla}^2 f_{+,\nu} = 2\zeta\epsilon_\nu f_{-,\nu} \tag{9}$$

$$-\zeta^2\tilde{\nabla}^2 f_{-,\nu} + 2f_{-,\nu} = 2\zeta\epsilon_\nu f_{+,\nu}. \tag{10}$$

The solutions can be written as $f_{\pm,\mathbf{m}} = C_{\pm,\mathbf{m}}W(\mathbf{m})$. Here we replaced the generic index ν by the vector index $\mathbf{m}$ that appears in the solutions. The prefactors have to be related as $C_{-,\mathbf{m}} = \zeta\epsilon_\mathbf{m}C_{+,\mathbf{m}}$, due to the normalization conditions on $u_\mathbf{m}$ and $v_\mathbf{m}$ (see Refs. [1,2]). The functions $W(\mathbf{m})$ are plane waves, $W(\mathbf{m}) = \exp(2\pi i\mathbf{m}\bar{\mathbf{r}})$, where $\mathbf{m} = (m_1, m_2, m_3)$, and m_1,m_2, and m_3 are integers. $\bar{\mathbf{r}}$ is defined as $\bar{\mathbf{r}} = (\bar{x}, \bar{y}, \bar{z})$. Eliminating $f_{-,\mathbf{m}}$ from Eqs. (9) and (10), we can obtain the low-momentum limit of an energy-momentum dispersion relationship:

$$-\tilde{\nabla}^2 f_{+,\mathbf{m}} = 2\epsilon_\mathbf{m}^2 f_{+,\mathbf{m}}. \tag{11}$$

Written in terms of the original parameters, this gives $E_\mathbf{m} = \hbar c|\mathbf{k}|$, where the phonon velocity is $c = \sqrt{gn_0/M}$, and $\mathbf{k}$ is defined as $\mathbf{k} = (2\pi m_1/X, 2\pi m_2/Y, 2\pi m_3/Z)$. The normalization of the BdG modes is given by $C_{+,\mathbf{m}}^2 = 2\mu/(E_\mathbf{m}V)$. In summary, the solutions of the BdG equations are

$$f_{+,\mathbf{m}} = \sqrt{\frac{2\mu}{VE_\mathbf{m}}}\exp(2\pi i\mathbf{m}\cdot\bar{\mathbf{r}}), \tag{12}$$

$$f_{-,\mathbf{m}} = \sqrt{\frac{E_\mathbf{m}}{V2\mu}}\exp(2\pi i\mathbf{m}\cdot\bar{\mathbf{r}}). \tag{13}$$

Within the weak interaction expansion used here, we have $\mu = gn_0$.

We now use these modes to calculate the correlation function of the phase. The phase field $\phi(\mathbf{r})$ is related to $f_{+,\mathbf{m}}$ through $\phi(\mathbf{r}) = 1/(2\sqrt{n_0})\sum_\mathbf{m} f_{+,\mathbf{m}}a_\mathbf{m}^\dagger + \text{H.c.}$, where $a_\mathbf{m}^\dagger$ is the bosonic creation operator of the $f_{+,\mathbf{m}}$ mode. The $f_{-,\mathbf{m}}$ modes, on the other hand, are related to the density fluctuations of the system. Because the modes $f_{+,\mathbf{m}}$ behave as $1/\sqrt{E_\mathbf{m}}$, whereas $f_{-,\mathbf{m}}$ scale as $\sqrt{E_\mathbf{m}}$, one can expect that at long distances (small k) the phase of the system can be a fluctuating quantity, whereas the density fluctuations will be suppressed.

The correlation function of the phase is given by

$$\langle\delta\phi(\mathbf{r})^2\rangle = \sum_\mathbf{m}\frac{g}{VE_\mathbf{m}}N_\mathbf{m}[2 - 2\cos(2\pi\mathbf{m}\cdot\bar{\mathbf{r}})], \tag{14}$$

where $\delta\phi(\mathbf{r}) \equiv \phi(0) - \phi(\mathbf{r})$. We assume that the Bogoliubov modes are occupied according to a Bose-Einstein distribution of temperature T. Thus, the distribution $N_\mathbf{m}$, which is the occupation of a state with energy $E_\mathbf{m}$, is given by

$$N_\mathbf{m} = \frac{1}{\exp(E_\mathbf{m}/k_BT) - 1} + 1/2, \tag{15}$$

where the $1/2$ accounts for the vacuum fluctuations. For small energies and at finite temperature, $N_\mathbf{m}$ has a divergent behavior, which is the origin of the phase-fluctuating regime. It behaves as

$$N_\mathbf{m} \approx \frac{k_BT}{E_\mathbf{m}}. \tag{16}$$

This divergent term dominates over the constant term $1/2$, which we discuss in Sec. II B. We find that it generates an algebraically decaying correlation function, with an exponent that is very small for the parameter regime of interest. In particular, the term does not contribute to the exponential decay, and will be ignored in this section.

A. Correlation function in 1D and 3D

The correlation function for the elongated geometry shows 3D behavior on short length scales $r \lesssim X,Y$, and 1D behavior for longer scales $r \gtrsim X,Y$. In this section we discuss these limits.

We first calculate the 3D limit by replacing the sums in Eq. (14) with integrals. The thermal contribution of the correlation function is

$$\langle\delta\phi(\mathbf{r})^2\rangle = \frac{g}{2\pi^2\hbar c}\left(\frac{\pi^2(k_BT)^2}{3\hbar^2c^2} + \frac{1}{r^2} - \frac{\pi k_BT\coth(\pi rk_BT/\hbar c)}{\hbar cr}\right), \tag{17}$$

where $r = |\mathbf{r}|$. For distances r large compared to the healing length $\xi = \hbar/(2Mgn_0)^{1/2}$ and the thermal de Broglie wavelength $\lambda = \hbar/(2\pi Mk_BT)^{1/2}$, this approaches

$$\langle \delta\phi(\mathbf{r})^2 \rangle \approx \frac{g}{2\pi^2\hbar c}\left(\frac{\pi^2(k_BT)^2}{3\hbar^2c^2} - \frac{\pi k_BT}{\hbar cr}\right), \tag{18}$$

(see, e.g., Ref. [21]). This expression shows the $1/r$ decay of the phase correlations of a 3D BEC to a nonzero value, related to the thermal depletion at $T \lesssim \mu$. The thermal depletion is proportional to $\xi/(n\lambda^4)$. Equation (18) is valid in the elongated geometry for $\xi,\lambda \ll r \lesssim X,Y$.

As we approach the 1D limit, for $r \gg X,Y$, the modes with $m_1 = m_2 = 0$ produce the dominant contribution to the correlation function, whereas the excited transverse modes provide corrections, which we discuss below. We write the correlation function as $\langle \delta\phi(\mathbf{r})^2 \rangle = \langle \delta\phi(\mathbf{r})^2 \rangle_0 + \langle \delta\phi(\mathbf{r})^2 \rangle_1$, where $\langle \delta\phi(\mathbf{r})^2 \rangle_0$ corresponds to the modes with $m_1 = m_2 = 0$, and $\langle \delta\phi(\mathbf{r})^2 \rangle_1$ to the remaining contributions in Eq. (14). For $\langle \delta\phi(\mathbf{r})^2 \rangle_0$, with the approximation in Eq. (16), we find

$$\langle \delta\phi(\mathbf{r})^2 \rangle_0 = \frac{gk_BT}{XY}\frac{Z}{(\hbar c)^2}(|\bar{z}| - \bar{z}^2). \tag{19}$$

In this expression, the linear term contains the length scale that we are interested in, whereas the quadratic term ensures that the derivative of the function at $\bar{z} = 1/2$ is smooth. One might expect an expression that is purely given by trigonometric functions of $\bar{z}$, however, the approximation in Eq. (16) leads to the expression above. We note that if we take the limit $Z \to \infty$, the linear term stays fixed, because it is only a function of z, whereas the quadratic term vanishes, because it scales as $1/Z$.

At intermediate distances $X,Y \ll r \ll Z$ (where the periodic boundary conditions are not apparent), the single-particle correlation function thus approaches

$$\langle \psi^\dagger(0)\psi(\mathbf{r}) \rangle \sim n_0 \exp(-Z|\bar{z}|/l_\phi), \tag{20}$$

where we used the phase-density representation of the boson operator $\psi(\mathbf{r}) = \sqrt{n(\mathbf{r})}\exp[i\phi(\mathbf{r})]$ to connect the single-particle correlation function to the phase-correlation function. The phase-correlation length l_ϕ is given by

$$l_\phi = \frac{2XY(\hbar c)^2}{gk_BT} = \frac{2XY\hbar^2 n_0}{Mk_BT} = \frac{2\hbar^2 N_0}{MZk_BT}. \tag{21}$$

We note that the interaction has canceled in this expression (see, e.g., Refs. [4,22]). This can be understood by writing the Hamiltonian in the phase-density representation. As discussed in Ref. [20], the Hamiltonian of a weakly interacting Bose gas is given to second order by a kinetic term $\sim n_0(\nabla\phi)^2/2M$ and a potential term of the form $g\delta n^2$, where δn are the density fluctuations around the constant value n_0. In the momentum representation, the spectrum of this Hamiltonian can be seen to be equivalent to the Bogoliubov spectrum of Eqs. (3) and (4). The contribution to the partition function made by a given mode of energy $\hbar\omega_k$ consists of independent phase and density terms, for a temperature $T \gtrsim \hbar\omega_k/k_B$. In this limit, the phase correlations are entirely due to the kinetic term, leading to the expression in Eq. (21), independent of the interaction strength.

Next, we estimate the effect of the higher modes, for the case $X = Y$. We consider the thermal contribution to the spatially independent part of the correlation function. We replace the m_3 summation in Eq. (14) by an integral over k_z, and expand the dispersion relation appearing in the exponent in Eq. (15) to second order in k_z. We can then evaluate the k_z integral as

$$\begin{aligned}\langle \delta\phi(\mathbf{r})^2 \rangle_1 &\approx \sum_{m_1,m_2\neq 0}\int \frac{dk_z}{2\pi}\frac{g}{\pi\hbar cX\left(m_1^2+m_2^2\right)^{1/2}}, \\ &\exp\left(-\frac{8\pi^2\hbar c\left(m_1^2+m_2^2\right)+\hbar cX^2k_z^2}{4\pi Xk_BT\left(m_1^2+m_2^2\right)^{1/2}}\right) \\ &= \sum_{m_1,m_2\neq 0}\frac{g}{\pi\hbar cX\left(m_1^2+m_2^2\right)^{1/4}}\left(\frac{k_BT}{X\hbar c}\right)^{1/2}, \\ &\exp\left(-\frac{2\pi\hbar c\left(m_1^2+m_2^2\right)^{1/2}}{Xk_BT}\right).\end{aligned} \tag{22}$$

Next we approximate the sum $\sum_{m_1,m_2\neq 0}$ by $\sum_{m=1}^{\infty} 2\pi m$, and $(m_1^2+m_2^2)^{1/2}$ by m. That gives

$$\begin{aligned}\langle \delta\phi(\mathbf{r})^2 \rangle_1 &\approx \sum_m \frac{2g\sqrt{m}}{\hbar cX}\left(\frac{k_BT}{X\hbar c}\right)^{1/2}\exp\left(-\frac{2\pi\hbar cm}{Xk_BT}\right) \\ &= \frac{2g(k_BT)^{1/2}}{(\hbar cX)^{3/2}}\mathrm{Li}_{-\frac{1}{2}}\left[\exp\left(-\frac{2\pi\hbar c}{Xk_BT}\right)\right],\end{aligned} \tag{23}$$

where $\mathrm{Li}_{-\frac{1}{2}}$ is the standard polylogarithmic function with exponent $-1/2$.

For temperatures large enough to populate transverse modes (i.e., $k_BT \gg 2\pi\hbar c/X$), but smaller than or comparable to μ, Eq. (23) becomes

$$\langle \delta\phi(\mathbf{r})^2 \rangle_1 \approx \frac{g(k_BT)^2}{2^{3/2}\pi(\hbar c)^3}. \tag{24}$$

We therefore approximately recover the 3D thermal depletion, which we found before in Eq. (18). For $k_BT \ll 2\pi\hbar c/X$, $\langle \delta\phi(\mathbf{r})^2 \rangle_1$ is exponentially suppressed,

$$\langle \delta\phi(\mathbf{r})^2 \rangle_1 \approx \frac{2g}{\hbar cX}\left(\frac{k_BT}{X\hbar c}\right)^{1/2}\exp\left(-\frac{2\pi\hbar c}{Xk_BT}\right). \tag{25}$$

In Fig. 1 we show the full thermal contribution to the correlation function, Eq. (14), for box dimensions $Z = 100$ μm and $X = Y = 5$ μm. The temperature is $T = 100$ nK, and the atomic mass is $M = 23u$, with u being the atomic mass unit. For $z \lesssim X,Y$ the correlation function $g_1(\mathbf{r})$ closely resembles the 3D result [see Eq. (17)] (i.e., it falls off on a short scale to a finite value), which describes the thermal depletion of the condensate. For sufficiently large $z \gg X,Y$, the correlation function $g_1(\mathbf{r})$ is approximately given by $g_1(z)$, and behaves like the correlation function for a 1D system. The thermally activated modes where $m_1,m_2 = 0$, $m_3 \neq 0$ generate an exponentially decaying $g_1(z)$. In this 1D-like case, the correlation function is essentially only a function of the coordinate z, and independent of x and y. The effect of the transverse modes is to create a constant thermal depletion, as in Eq. (24), which is of the order of the 3D result. So the crossover from 3D to 1D is given by the geometric shape, and the regimes are $z \lesssim X,Y$ for 3D behavior, and $z \gtrsim X,Y$ for 1D behavior (see also Ref. [23]).

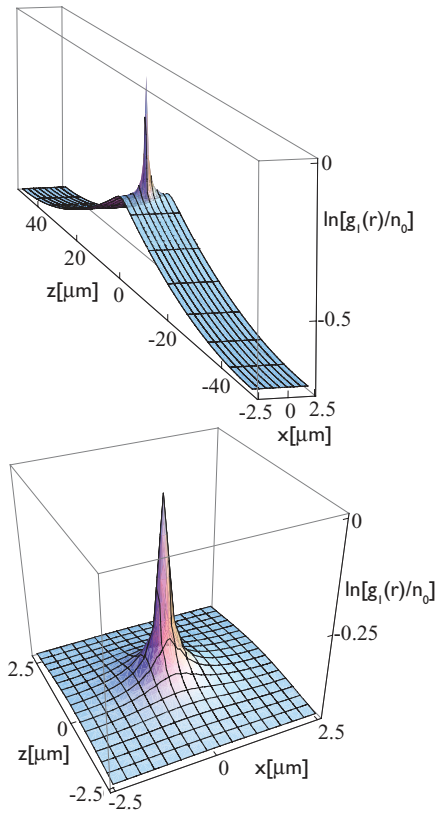

FIG. 1. (Color online) Thermal contribution to the correlation function $g_1(\mathbf{r}) = \langle\psi^\dagger(0)\psi(\mathbf{r})\rangle$. We plot $\ln(\langle\psi^\dagger(0)\psi(\mathbf{r})\rangle/n_0)$, which equals $-\langle\delta\phi(\mathbf{r})^2\rangle/2$. We use a box geometry with $Z = 100$ μm and $X = Y = 5$ μm, and a temperature $T = 100$ nK. The total atom number is $N_0 = 20\,000$, and M is the sodium mass $M = 23u$, with u being the atomic mass unit. We assume that the scattering length is $a = 2.75$ nm. The top diagram shows the full correlation function, the bottom diagram the regime $z \lesssim X, Y$.

B. Phase-fluctuating condensate

In the previous section we found that for an elongated system the long-range behavior of the single-particle correlation function $g_1(\mathbf{r})$ shows exponential decay with a correlation length l_ϕ. We can then define a temperature above which the system is in the phase-fluctuating regime, based on the requirement that this length scale is comparable to the system size (i.e., $l_\phi \approx Z$). This defines the following temperature:

$$k_B T_\phi = \frac{2\hbar^2 N_0}{M Z^2}. \tag{26}$$

If this temperature lies below the BEC temperature T_c, a phase-fluctuating condensate may exist. We estimate that temperature by using the result for the homogeneous, ideal Bose gas, which is (e.g., Ref. [24])

$$k_B T_c = \frac{2\pi}{\zeta(3/2)^{2/3}} \frac{\hbar^2 n_0^{2/3}}{M}, \tag{27}$$

where ζ signifies the Riemann zeta function. To estimate the regime in which one would observe a phase-fluctuating condensate, we consider the ratio of T_c and T_ϕ,

$$T_c/T_\phi = \frac{\pi}{\zeta(3/2)^{2/3}} \frac{1}{N_0^{1/3}} \frac{Z^{4/3}}{X^{4/3}}, \tag{28}$$

which we wrote in terms of the total atom number N_0, and we chose $X = Y$. For a system of fixed dimensions X and Z, no phase-fluctuating regime exists if the total number of atoms fulfills

$$N_0 \gtrsim \frac{\pi^3}{\zeta(3/2)^2} \frac{Z^4}{X^4} \approx 4.5 \frac{Z^4}{X^4}, \tag{29}$$

demonstrating how sensitively the presence or absence depends on the geometric ratio Z/X. In Fig. 2 we show both the condensate temperature and T_ϕ as a function of density, for different geometric dimensions. The regime above T_ϕ but below T_c is the phase-fluctuating condensate regime. We can again see that the magnitude of this regime is very sensitive to the ratio Z/X.

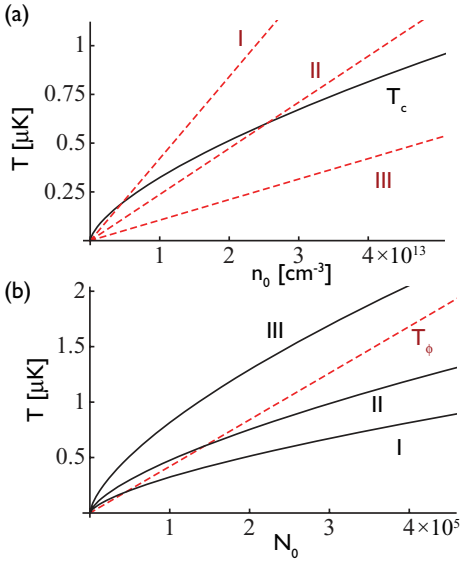

FIG. 2. (Color online) Comparison of T_c (black, solid lines) and T_ϕ (red, dashed lines), for different geometric aspect ratios. In (a) we show these temperatures as a function of density, for the sodium mass $M = 23u$, and $Z = 100$ μm, and for $X = Y = 10, 7.5, 5$ μm (I–III). In (b) we show the same quantities as a function of the total atom number N_0. T_c is purely a function of the density, whereas T_ϕ is a function of the total number, for a fixed longitudinal dimension Z.

II. RING GEOMETRY

We now turn to the kind of ring-shaped geometry in which we are interested. As mentioned in Sec. I, we will find that qualitatively most features of the phase-fluctuating condensate in a ring can be understood in terms of the simplified box geometry discussed previously. We note that the elongated box with periodic boundary condition is very similar to a ring. In addition, the cigar-shaped condensates discussed in Refs. [1,2] qualitatively share similar features in the center of the condensate. In this section, we derive the results analogous to those of the previous section but for a trapped (inhomogeneous) ring system and compare them to results of Sec. I.

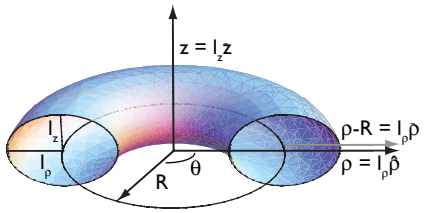

FIG. 3. (Color online) The toroidal shape of the BEC is given by the radius R, and the Thomas-Fermi radii l_z in z direction, and l_ρ in radial direction. We use the rescaled z variable $\bar{z} = z/l_z$, and the two rescaled radial variables $\hat{\rho} = \rho/l_\rho$ and $\bar{\rho} = (\rho - R)/l_\rho$, as indicated in the figure.

In the treatment here, the trapping potential is approximated by the harmonic form,

$$V = \tfrac{1}{2}M\omega_z^2 z^2 + \tfrac{1}{2}M\omega_\rho^2(\rho - R)^2. \tag{30}$$

Here, z and ρ are spatial cylindrical coordinates as shown in Fig. 3, and ω_z and ω_ρ the oscillation frequencies along the spatial directions, and R is the mean ring radius. We apply the same formalism as in Sec. I. The GP equation of the system is given by

$$\left(-\frac{\hbar^2\nabla^2}{2M} + V + g|\Psi_0|^2\right)\Psi_0 = \mu\Psi_0, \tag{31}$$

the BdG equations are

$$\left(-\frac{\hbar^2\nabla^2}{2M} + V\right)u_\nu + g|\Psi_0|^2(2u_\nu - v_\nu) = (\mu + E_\nu)u_\nu, \tag{32}$$

$$\left(-\frac{\hbar^2\nabla^2}{2M} + V\right)v_\nu + g|\Psi_0|^2(2v_\nu - u_\nu) = (\mu - E_\nu)v_\nu. \tag{33}$$

The Thomas-Fermi (TF) solution of Eq. (31) for $\bar{z}^2 + \bar{\rho}^2 < 1$ is

$$\Psi_0 = \sqrt{n_{\max}(1 - \bar{z}^2 - \bar{\rho}^2)}. \tag{34}$$

Here we have rescaled the spatial coordinates $\bar{z} = z/l_z$ and $\bar{\rho} = (\rho - R)/l_\rho$ by the TF radii, given by $l_z = (2\mu/M\omega_z^2)^{1/2}$ and $l_\rho = (2\mu/M\omega_\rho^2)^{1/2}$. This rescaling is in analogy to rescaling the spatial coordinates of the box geometry by the dimensions of the box. $n_{\max}$ is the maximum value of the density of the condensate. We write the GP equation as

$$-\eta^2\tilde{\nabla}^2\Psi_0 + \bar{z}^2\Psi_0 + \bar{\rho}^2\Psi_0 + \bar{n}_0\Psi_0 = \Psi_0, \tag{35}$$

where we introduced the operator,

$$\tilde{\nabla}^2 = \left[\frac{\omega_\rho^2}{\bar{\omega}^2}\left(\frac{\partial^2}{\partial\hat{\rho}^2} + \frac{1}{\hat{\rho}}\frac{\partial}{\partial\hat{\rho}} + \frac{1}{\hat{\rho}^2}\frac{\partial^2}{\partial\theta^2}\right) + \frac{\omega_z^2}{\bar{\omega}^2}\frac{\partial^2}{\partial\bar{z}^2}\right], \tag{36}$$

where θ is the azimuthal angle, as shown in Fig. 3, and $\hat{\rho} = \rho/l_\rho$. The frequency $\bar{\omega} = \sqrt{\omega_z\omega_\rho}$, and $\eta^2 = \frac{\hbar\bar{\omega}}{2\mu}$ [25].

We now introduce a rescaled energy $\epsilon_\nu = E_\nu/\hbar\bar{\omega}$ and a rescaled density $\bar{n}_0$, defined as $\bar{n}_0 = |\Psi_0|^2/n_{\max}$. With these parameters, the BdG equations are

$$-\eta^2\tilde{\nabla}^2 u_\nu + (\bar{z}^2 + \bar{\rho}^2)u_\nu + (2u_\nu - v_\nu)\bar{n}_0 = (1 + 2\eta\epsilon_\nu)u_\nu, \tag{37}$$

$$-\eta^2\tilde{\nabla}^2 v_\nu + (\bar{z}^2 + \bar{\rho}^2)v_\nu + (2v_\nu - u_\nu)\bar{n}_0 = (1 - 2\eta\epsilon_\nu)v_\nu. \tag{38}$$

These equations are analogous to Eqs. (7) and (8), but here the equations contain a spatially dependent potential and condensate density $\bar{n}_0 = \bar{n}_0(\bar{z}, \bar{\rho})$.

As before, we introduce the fields $f_{\pm,\nu} = u_\nu \pm v_\nu$. In terms of these, the BdG equations are

$$\left(-\eta^2\tilde{\nabla}^2 + \frac{\eta^2\tilde{\nabla}^2\Psi_0}{\Psi_0}\right)f_{+,\nu} = 2\eta\epsilon_\nu f_{-,\nu}, \tag{39}$$

$$\left(-\eta^2\tilde{\nabla}^2 + 2 - 2\bar{z}^2 - 2\bar{\rho}^2 + \frac{3\eta^2\tilde{\nabla}^2\Psi_0}{\Psi_0}\right)f_{-,\nu} = 2\eta\epsilon_\nu f_{+,\nu} \tag{40}$$

We write the solutions in the TF approximation as

$$f_{+,\nu} = C_{+,\nu}(1 - \bar{z}^2 - \bar{\rho}^2)^{1/2}W_\nu(\theta), \tag{41}$$

$$f_{-,\nu} = C_{-,\nu}(1 - \bar{z}^2 - \bar{\rho}^2)^{-1/2}W_\nu(\theta), \tag{42}$$

with the normalization condition $C_{-,\nu} = \eta\epsilon_\nu C_{+,\nu}$. The functions $W_\nu(\theta)$ are simply $W_\nu = \exp(im\theta)$, with m being an integer. We replace the index ν with m from now on. For these solutions we assumed that the radius R is much larger than l_ρ, so that we can approximate the term $(1/\hat{\rho}^2)\partial_\theta^2$ in Eq. (36) by $(l_\rho^2/R^2)\partial_\theta^2$.

This set of modes is analogous to the modes with $m_1 = m_2 = 0$ in the previous section. In analogy to Eq. (11), the dispersion relation can be calculated from

$$(1 - \bar{z}^2 - \bar{\rho}^2)\left(-\tilde{\nabla}^2 + \frac{\tilde{\nabla}^2\Psi_0}{\Psi_0}\right)f_{+,m} = 2\epsilon_m^2 f_{+,m}, \tag{43}$$

where we need to average over the density profile (see Refs. [1,26]). This gives $E_m = \hbar c|k|$, with $c = \sqrt{gn_{\max}/2M}$ and $k = m/R$. These modes and dispersion relation were also discussed within a hydrodynamic approach in Ref. [26]. The prefactor $C_{+,m}$ is given by $C_{+,m}^2 = 1/(2\pi^2\epsilon_m\eta Rl_z l_\rho)$, so $f_{\pm,m}$ are

$$f_{+,m} = \sqrt{\frac{gn_0(z,\rho)}{\pi^2 Rl_z l_\rho E_m}}\exp(im\theta), \tag{44}$$

$$f_{-,m} = \sqrt{\frac{E_m}{4\pi^2 Rl_z l_\rho g n_0(z,\rho)}}\exp(im\theta). \tag{45}$$

These expressions are analogous to Eqs. (12) and (13). The "Thomas-Fermi" volume V in Eqs. (12) and (13) corresponds to $2\pi^2 Rl_z l_\rho$, which is the volume of the torus. The chemical potential μ is replaced by $gn_0(\rho, z)$.

Next, we calculate the correlation function of the phase,

$$\langle\delta\phi(\theta)^2\rangle = \sum_m \frac{gN_m}{2\pi^2 Rl_z l_\rho E_m}[2 - 2\cos(m\theta)], \tag{46}$$

where N_m is given in Eq. (15). In analogy with $\delta\phi(\mathbf{r})$ in the previous section, we have defined $\delta\phi(\theta) = \phi(0) - \phi(\theta)$. Using Eq. (16), we find

$$\langle\delta\phi(\theta)^2\rangle = \frac{gk_BT}{\pi^2 l_z l_\rho}\frac{R}{(\hbar c)^2}(-\theta^2/2 + \pi|\theta|), \tag{47}$$

in analogy to Eq. (19). So for intermediate distances $l_\rho, l_z \ll R\theta \ll R$ we have $\langle\psi^\dagger(\theta)\psi(\theta')\rangle \sim \exp(-R|\Delta\theta|/l_\phi)$, with

$$l_\phi = \frac{\pi l_z l_\rho \hbar^2 n_{\max}}{M k_B T} = \frac{\hbar^2 N_0}{\pi M R k_B T}, \tag{48}$$

in analogy to Eq. (20). Here we used the relationship between the density maximum $n_{\max}$ and the total atom number N_0, $N_0 = n_{\max}\pi^2 l_z l_\rho R$. Again we find that the interaction does not affect l_ϕ. We note that this expression is of the same form as the expression for the box geometry, Eq. (21), up to numerical prefactors.

A. Phase-fluctuating regime

As in Sec. I, the phase-fluctuating regime is reached when the phase-correlation length is of the order of the system size. From $l_\phi \approx \pi R$ we can define the temperature,

$$k_B T_\phi = \frac{\hbar^2 N_0}{\pi^2 M R^2}. \tag{49}$$

We calculate the condensation temperature for a cylinder of length $2\pi R$ and with harmonic confinement with frequencies ω_z and ω_ρ,

$$k_B T_c = \left(\frac{3 N_0 \hbar^3 \omega_z \omega_\rho}{4\Gamma(\alpha)\zeta(\alpha)(2m)^{1/2} R}\right)^{2/5}, \tag{50}$$

where $\zeta(\alpha)$ is again the Riemann function at $\alpha = 5/2$, and $\Gamma(\alpha)$ is the usual Gamma function.

As discussed in Ref. [27], at this critical temperature the density at the potential minimum reaches the critical value of the homogeneous system, within a semiclassical approximation.

The ratio T_c/T_ϕ can be written as

$$\frac{T_c}{T_\phi} = \left(\frac{3\pi^5}{4\sqrt{2}\Gamma(\alpha)\zeta(\alpha)}\right)^{2/5} \frac{1}{N_0^{3/5}} \left(\frac{R^2}{a_z a_\rho}\right)^{4/5}, \tag{51}$$

where $a_z = \sqrt{\hbar/m\omega_z}$ and $a_\rho = \sqrt{\hbar/m\omega_\rho}$ are the oscillator lengths of the confining potential. For the total atom number this leads to the inequality,

$$N_0 \gtrsim \left(\frac{3\pi^5}{4\sqrt{2}\Gamma(\alpha)\zeta(\alpha)}\right)^{2/3} \left(\frac{R^2}{a_z a_\rho}\right)^{4/3} \tag{52}$$

$$\approx 20.2 \left(\frac{R^2}{a_z a_\rho}\right)^{4/3}, \tag{53}$$

for which there is no phase-fluctuating condensate for any temperature. This conclusion is valid if the estimate of the condensate temperature in Eq. (50) is accurate, and under the weak interaction conditions of the BdG approach.

In Fig. 4 we show T_ϕ and T_c as a function of the total atom number N_0, and for different confining frequencies ω_z and ω_ρ. For a given N_0 and trap radius R, T_ϕ is fixed. The condensation temperature, however, is affected by the transverse confinement through ω_z and ω_ρ. By increasing their value, a large regime of a phase-fluctuating condensate can be created. On the other hand, for sufficiently weak transverse confinement, one can avoid the phase fluctuating regime for all temperatures.

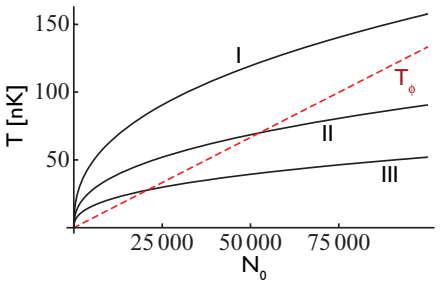

FIG. 4. (Color online) T_ϕ (red, dashed line) as a function of the total atom number, for $M = 23u$ and $R = 40$ μm, and T_c (black, solid lines) for $\omega_z = \omega_\rho = 2\pi \times 200, 2\pi \times 100, 2\pi \times 50$ Hz (I–III).

B. Zero temperature

While one might expect that in 3D a condensate would have perfect phase coherence at zero temperature, we find that the phase-fluctuating character of an elongated system persists even at zero temperature, as for a truly 1D system [28]. At zero temperature, the single-particle correlation function of our ring-shaped condensate decays algebraically:

$$\langle\psi^\dagger(\mathbf{r}_1)\psi(\mathbf{r}_2)\rangle \sim \left(\frac{(R\theta)^2}{r_c^2}\right)^{-1/4K}, \tag{54}$$

where $\mathbf{r}_1$ and $\mathbf{r}_2$ both are at the minimum of the trapping potential, with $|\mathbf{r}_1| = |\mathbf{r}_2| = R$, and θ is the angle between them. Equation (54) is valid for $l_z, l_\rho, r_c \ll |R\theta| \ll R$, where r_c is a short-range cutoff which should be chosen to be of the order of the healing length $l_h = \frac{\hbar}{\sqrt{m\mu}}$, see [29].

The scaling exponent K is given by

$$K = \frac{\hbar N_0^{3/4}}{2^{1/4} R^{3/4} M^{3/4}} \frac{\pi^{1/2}}{g^{1/4}(\omega_z\omega_\rho)^{1/4}}. \tag{55}$$

For typical parameters, K is very large. For example, for $R = 40$ μm, $M = 23u$, $a = 2.75$ nm, $\omega_z = \omega_\rho = 2\pi \times 1000$ Hz, and $N_0 = 20\,000$, we have $K = 242.4$. Since the algebraically decaying correlation function reaches, say, the value $1/e$ at a distance $r_c e^{2K}$, which vastly exceeds the size of the system, the decay of the correlation function across the system is very small. So although the system in principle forms a quasicondensate, for typical parameters it will behave essentially like a true condensate.

III. EXPERIMENTAL SIGNATURES

In this section we consider possible experimental signatures of the phase-fluctuating regime. The defining feature of this regime is the loss of phase coherence over the ring-shaped condensate. One way of testing this would be to use the interference technique demonstrated in Ref. [11].

In Ref. [6] the signature of the phase-fluctuating regime in time-of-flight images was studied. In Ref. [7] an interferometric approach measuring the second-order correlation function was reported. In Ref. [9] Bragg spectroscopy was used to measure the momentum distribution in the axial direction, which was calculated in Ref. [8]. Matter wave interferometry was used in Ref. [10] to measure the phase-coherence length.

A consequence of the ring geometry is that during a time-of-flight (TOF) expansion of the phase-fluctuating condensate, the contrast of matter-wave interference should be reduced compared to a true condensate. In particular, due to the ring-shaped geometry of the system one can expect that the constructive interference that can emerge at the center of the ring during expansion will be reduced.

We now discuss the interference of atoms released from a ring trap. For this purpose we use a Green's function approach which conveniently relates the density after time of flight to the two-field correlation function prior to release. Assuming freely expanding atoms, the time-dependent bosonic single-particle annihilation operator is given by

$$\psi(\mathbf{x},t) = \int d\mathbf{x}_1 w(\mathbf{x}-\mathbf{x}_1,t)\psi(\mathbf{x}_1). \tag{56}$$

Here, $\psi(\mathbf{x},t)$ is the bosonic single-particle annihilation operator at time t, and $\psi(\mathbf{x}_1)$ is the initial single-particle operator. The Green's function of free propagation $w(\mathbf{x},t)$ is given by

$$w(\mathbf{x},t) = \left(\frac{M}{2\pi i\hbar t}\right)^{3/2} \exp(iM\mathbf{x}^2/2\hbar t). \tag{57}$$

The expectation of the density at time t is, therefore,

$$n(\mathbf{x},t) = \iint d\mathbf{x}_1 d\mathbf{x}_2 w^*(\bar{\mathbf{x}}_1,t)w(\bar{\mathbf{x}}_2,t)\langle\psi^\dagger(\mathbf{x}_1)\psi(\mathbf{x}_2)\rangle, \tag{58}$$

with $\bar{\mathbf{x}}_1 = \mathbf{x}-\mathbf{x}_1$ and $\bar{\mathbf{x}}_2 = \mathbf{x}-\mathbf{x}_2$. We are interested in the density integrated over the z direction, and we switch to cylindrical coordinates:

$$n(\rho,t) = \int dz\, n(\rho,z,t). \tag{59}$$

Using Eq. (58), and integrating over z, we find

$$\begin{aligned} n(\rho,t) = \left(\frac{M}{2\pi\hbar t}\right)^3 \frac{\hbar t}{M} \int dz_1 \rho_1\, d\rho_1 \rho_2\, d\rho_2\, d\theta_1\, d\theta_2, \\ \exp\left\{iM[\rho(\rho_1\cos\theta_1 - \rho_2\cos\theta_2)]/\hbar t \right. \\ \left. - iM\left(\rho_1^2-\rho_2^2\right)/2\hbar t\right\}\sqrt{n(\rho_1,z_1)n(\rho_2,z_1)}, \\ \exp\{-R/l_\phi[|\Delta\theta| - (\Delta\theta)^2/2\pi]\}. \end{aligned} \tag{60}$$

Here we assumed that the single-particle correlation function is of the form,

$$\begin{aligned} &\langle\psi^\dagger(\rho_1,z_1,\theta_1)\psi(\rho_2,z_2,\theta_2)\rangle \\ &\quad = \sqrt{n(\rho_1,z_1)n(\rho_2,z_1)}\exp\left[\frac{R}{l_\phi}\left(\frac{\Delta\theta^2}{2\pi} - |\Delta\theta|\right)\right], \end{aligned} \tag{61}$$

with $\Delta\theta = \theta_1 - \theta_2$. Here we have ignored the condensate depletion due to thermal activation of transverse modes.

We perform the integral of Eq. (60) using shifted coordinates $\tilde{\rho}_1$ and $\tilde{\rho}_2$, defined by $\rho_1 = R+\tilde{\rho}_1$ and $\rho_2 = R+\tilde{\rho}_2$. Ignoring quadratic terms in $\tilde{\rho}_{1,2}$ in the exponent we obtain

$$\begin{aligned} n(\rho,t) \approx \frac{n_{\max}}{4} \int dz_1\, d\theta_1 d\theta_2 A^*(\theta_1)A(\theta_2), \\ \exp[iM\rho R(\cos\theta_1 - \cos\theta_2)/\hbar t], \\ \exp\{-R/l_\phi[|\Delta\theta| - (\Delta\theta)^2/2\pi]\}, \end{aligned} \tag{62}$$

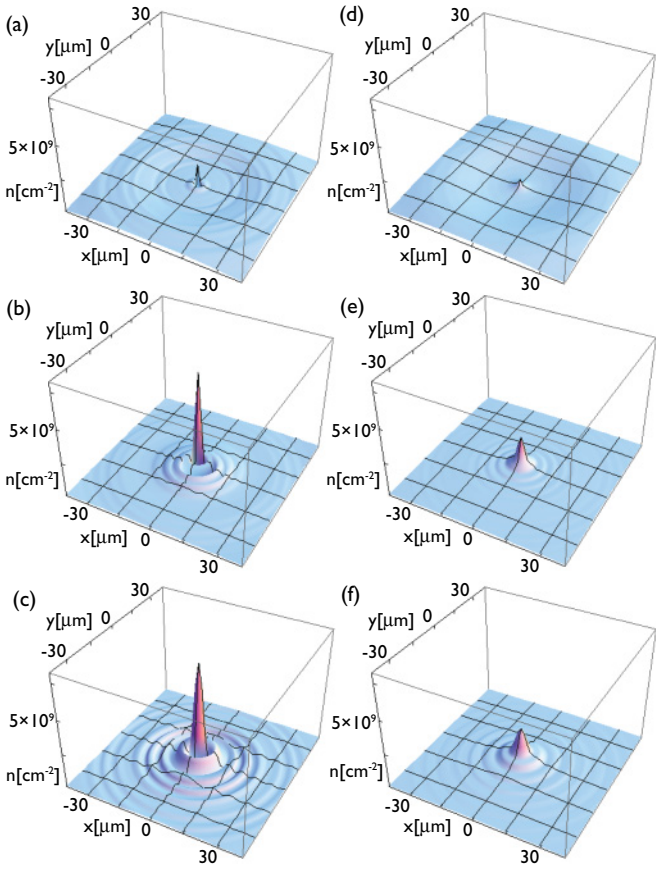

FIG. 5. (Color online) Expectation value of the density, integrated over the z direction, after time-of-flight expansion of an atomic ensemble of $N_0 = 30\,000$ atoms of mass $M = 23u$, in a ring with radius $R = 40\ \mu$m, and $\omega_z = 2\pi \times 1000$ Hz and $\omega_\rho = 2\pi \times 200$ Hz. (a)–(c) The TOF interference for $T = 20$ nK, at times $t = 10,20,30$ ms. (d)–(f) TOF interference for $T = 170$ nK at the same times.

where $A(\theta)$ is given by

$$\begin{aligned} A(\theta) = \frac{1}{(R-\rho\cos\theta)} \\ \times\left\{R\sqrt{1-z_1^2/l_z^2}, J_1\left[\frac{Ml_\rho\sqrt{1-z_1^2/l_z^2}(R-\rho\cos\theta)}{\hbar t}\right]\right. \\ + il_\rho\left(1-z_1^2/l_z^2\right), \\ \left. J_2\left[\frac{Ml_\rho\sqrt{1-z_1^2/l_z^2}(R-\rho\cos\theta)}{\hbar t}\right]\right\}. \end{aligned} \tag{63}$$

We evaluate Eq. (62) numerically, for $R = 40$ nm, $N_0 = 30\,000$, $\omega_z = 2\pi \times 1000$ Hz, and $\omega_\rho = 2\pi \times 200$ Hz. We assume M to be the sodium mass, $M = 23u$, where u is the atomic mass unit, and $a = 2.75$ nm. We note again that in this example the interactions are taken into account for the initial state, whereas the time-of-flight expansion is ballistic. The initial velocity distribution is given by the TF wave function in the transverse direction and by the thermal distribution of the phononic modes along the longitudinal direction.

In Figs. 5(a)–5(c) we show the case of $T = 20$ nK, at times $t = 10, 20, 30$ ms, in Figs. 5(d)–5(f) the case of $T = 170$ nK for the same times. The latter is in the phase-fluctuating regime and the contrast of the expectation value of the density is visibly reduced. In particular, the density at the center varies with time as

$$n(0,t) \approx \frac{\pi n_{\max}}{2} F(l_\phi) \int_{-l_z}^{l_z} dz \left(1 - z^2/l_z^2\right), \\ J_1^2\left(M l_\rho \sqrt{1 - z^2/l_z^2}\, R/\hbar t\right), \tag{64}$$

where

$$F(l_\phi) = \pi \sqrt{\frac{2l_\phi}{R}} \exp(-\pi R/2l_\phi) \mathrm{erf}_i(\sqrt{\pi R/2l_\phi}) \tag{65}$$

is a measure of phase coherence around the ring.

For small l_ϕ/R, $F(l_\phi)$ behaves as $F(l_\phi) \approx 2l_\phi/R$. For large values of l_ϕ/R, it saturates to $F(l_\phi) = 2\pi$. This behavior of the overall scale of the interference directly reflects the phase coherence of the BEC. The more coherent the system is, the higher the interference contrast of the time-of-flight image.

At short times $n(0,t)$ shows a linear behavior in time, when time averaged over the fast oscillatory behavior:

$$n(0,t) \approx \frac{\pi n_{\max}}{2} F(l_\phi) \frac{\hbar t l_z}{2 M l_\rho R}. \tag{66}$$

At long times $n(0,t)$ falls off as $\sim 1/t^2$:

$$n(0,t) \approx \frac{\pi n_{\max}}{2} F(l_\phi) \left(\frac{M l_\rho R}{\hbar t}\right)^2 \frac{4 l_z}{15}. \tag{67}$$

By comparing Eqs. (66) and (67) we can see that the time at which the center density is maximum scales as $t_{\max} \sim R/[\hbar/(l_\rho M)]$. The radius R is the distance traveled, and $\hbar/(l_\rho M)$ is the scale of the velocity distribution in radial direction.

We note that the expansion of a repulsively interacting gas should be faster than that of a noninteracting one, because the potential energy of the initial state is transformed into kinetic energy. The main observation, however, that a phase-coherent sample would show constructive interference at the center of the ring, whereas an incoherent sample would not, should still apply. However, the increased atomic velocity would lead to smaller fringe spacings making optical resolution of the narrow central peak more difficult. For sufficiently small interactions and for high enough optical resolution, this method could nevertheless constitute a method to detect the phase-fluctuating regime.

IV. CONCLUSIONS

We have studied the phase-fluctuating regime of condensates in a ring-shaped trap. We first considered a simplified box geometry in Sec. I, and calculated the properties of the phase-correlation function. We then turned to a realistic ring geometry in Sec. II. The main results are the estimates of the T_ϕ in Eq. (49), and of T_c in Eq. (50). With these expressions, one can determine whether the phase-fluctuating regime can be reached, as shown in Fig. 4. We present a simple condition, depending only on atom number and trap aspect ratio, that guarantees avoidance of the phase fluctuating regime for all temperature below T_c. We also discussed observing the regime of phase fluctuations in time-of-flight images.

ACKNOWLEDGMENTS

This work was supported by the National Science Foundation under Physics Frontier Grant No. PHY-0822671. L.M. acknowledges support from the National Research Council (NRC)/NIST.

[1] D. S. Petrov, G. V. Shlyapnikov, and J. T. M. Walraven, Phys. Rev. Lett. **87**, 050404 (2001).
[2] P. Öhberg, E. L. Surkov, I. Tittonen, S. Stenholm, M. Wilkens, and G. V. Shlyapnikov, Phys. Rev. A **56**, R3346 (1997).
[3] U. Al Khawaja, N. P. Proukakis, J. O. Andersen, M. W. J. Romans, and H. T. C. Stoof, Phys. Rev. A **68**, 043603 (2003).
[4] F. Gerbier, Europhys. Lett. **66**, 771 (2004).
[5] N. J. van Druten and W. Ketterle, Phys. Rev. Lett. **79**, 549 (1997).
[6] S. Dettmer *et al.*, Phys. Rev. Lett. **87**, 160406 (2001).
[7] D. Hellweg, L. Cacciapuoti, M. Kottke, T. Schulte, K. Sengstock, W. Ertmer, and J. J. Arlt, Phys. Rev. Lett. **91**, 010406 (2003).
[8] F. Gerbier, J. H. Thywissen, S. Richard, M. Hugbart, P. Bouyer, and A. Aspect, Phys. Rev. A **67**, 051602(R) (2003).
[9] S. Richard, F. Gerbier, J. H. Thywissen, M. Hugbart, P. Bouyer, and A. Aspect, Phys. Rev. Lett. **91**, 010405 (2003).
[10] M. Hugbart, J. A. Retter, F. Gerbier, A. F. Varon, S. Richard, J. H. Thywissen, D. Clement, P. Bouyer, and A. Aspect, Eur. Phys. J. D **35**, 155 (2005).
[11] P. Cladé, C. Ryu, A. Ramanathan, K. Helmerson, and W. D. Phillips, Phys. Rev. Lett. **102**, 170401 (2009).
[12] The experimental setup will be discussed in detail elsewhere.
[13] C. Ryu, M. F. Andersen, P. Cladé, V. Natarajan, K. Helmerson, and W. D. Phillips, Phys. Rev. Lett. **99**, 260401 (2007).
[14] K. Henderson, C. Ryu, C. MacCormick, and M. G. Boshier, New J. Phys. **11**, 043030 (2009).
[15] O. Morizot, Y. Colombe, V. Lorent, H. Perrin, and B. M. Garraway, Phys. Rev. A **74**, 023617 (2006).
[16] S. Muniz and C. Raman (unpublished).
[17] E. P. Gross, Nuovo Cimento **20**, 3 (1961); L. P. Pitaevskii, Sov. Phys. JETP **13**, 2 (1961).
[18] F. Dalfovo, S. Giorgini, L. Pitaevskii, and S. Stringari, Rev. Mod. Phys. **71**, 463 (1999).
[19] P. G. de Gennes, *Superconductivity of Metals and Alloys* (Benjamin, New York, 1966).
[20] C. Mora and Y. Castin, Phys. Rev. A **67**, 053615 (2003).
[21] T. M. Rice, Phys. Rev. **140**, A1889 (1965).
[22] M. A. Cazalilla, J. Phys. B: At. Mol. Opt. Phys. **37**, S1 (2004).
[23] H.-J. Mikeska and H. Schmidt, J. Low Temp. Phys. **2**, 371 (1970).

[24] C. J. Pethick and H. Smith, *Bose-Einstein Condensation in Dilute Gases* (Cambridge Press, Cambridge, 2002).

[25] The parameter η is similar to the parameter ζ defined for Eq. (5), but includes only the transverse dimensions in the rescaling, whereas ζ includes all three dimensions, in analogy to Ref. [2].

[26] S. Stringari, Phys. Rev. A **58**, 2385 (1998).

[27] V. Bagnato, D. E. Pritchard, and D. Kleppner, Phys. Rev. A **35**, 4354 (1987).

[28] T. Giamarchi, *Quantum Physics in One Dimension* (Oxford University Press, Oxford, 2004).

[29] The Bogoliubov spectrum crosses from a linear spectrum over to a quadratic spectrum at the inverse healing length. This motivates the choice of the healing length as a short-range cutoff. This short-range cutoff also appears in the long-range behavior of the correlation function, as the smallest "unit" of the spatial variables, which is characteristic for low-dimenionsal systems.